JPE 16-2-28

http://dx.doi.org/10.6113/JPE.2016.16.2.685
ISSN(Print): 1598-2092 / ISSN(Online): 2093-4718

A Reliability Evaluation Model for the Power Devices Used in Power Converter Systems Considering the Effect of the Different Time Scales of the Wind Speed Profile

Haiting Ji[†], Hui Li[*], Yang Li[*], Li Yang[**], Guoping Lei[**], Hongwei Xiao[*], Jie Zhao[*], and Lefeng Shi[***]

[†,**]Key Laboratory of Signal and Information Processing, Chongqing Three Gorges University, Chongqing, China
[*]State Key Laboratory of Power Transmission Equipment, System Security and New Technology, School of Electrical Engineering, Chongqing University, Chongqing, China
[***]Research Institute of Chongqing Electric Power, Chongqing, China

Abstract

This paper presents a reliability assessment model for the power semiconductors used in wind turbine power converters. In this study, the thermal loadings at different timescales of wind speed are considered. First, in order to address the influence of long-term thermal cycling caused by variations in wind speed, the power converter operation state is partitioned into different phases in terms of average wind speed and wind turbulence. Therefore, the contributions can be considered separately. Then, in regards to the reliability assessment caused by short-term thermal cycling, the wind profile is converted to a wind speed distribution, and the contribution of different wind speeds to the final failure rate is accumulated. Finally, the reliability of an actual power converter semiconductor for a 2.5 MW wind turbine is assessed, and the failure rates induced by different timescale thermal behavior patterns are compared. The effects of various parameters such as cut-in, rated, cut-out wind speed on the failure rate of power devices are also analyzed based on the proposed model.

Key words: Reliability evaluation, Thermal loading, Time scale, Wind farm, Wind Turbine Power Converter System (WTPCS)

I. INTRODUCTION

Wind Turbine Power Converter Systems (WTPCSs) are critical in terms of the reliable operation of wind energy conversion systems (WECS). According to market feedback, WTPCSs are more prone to failure than generators and gearboxes [1]. Surveys also indicate that WTPCSs and their power semiconductors vary significantly in terms of failure rates depending on the WTPCS topologies and operating environments. Tavner et al. [2], [3] suggest that both the average wind speed and wind turbulence significantly affect the reliability of WTPCS power devices based on several statistical analyses. Nonetheless, the effects of wind turbulence on the reliability of WTPCS power devices has not gained adequate attention. Hence, a reliability assessment that considers the effect of average wind speed and wind turbulence intensity in such devices is essential.

Studies on the reliability of the power devices used in wind power converters can be categorized into two main classes:

1) Statistical approaches, which are difficult to apply if the statistical data on failure is insufficient [2], [3].
2) Physical-of-failure based approach, which considers almost all of the physical stresses, e.g. wind speed, wind turbulence, operation model or environment temperature that can result in power device failure [5]-[8].

The failure mechanism caused by these physical stresses

Manuscript received May 28, 2015; accepted Nov. 16, 2015
Recommended for publication by Associate Editor Dong-Myung Lee.
[†]Corresponding Author: haitingji@163.com
Tel: +86-15223495819, Chongqing Three Gorges University
[*]State Key Laboratory of Power Transmission Equipment and System Security and New Technology, China
[**]Key Laboratory of Signal and Information Processing, Chongqing Three Gorges University, China
[***]Research Institute of Chongqing Electric Power, China

can be traced as thermomec fatigue stresses which is the dominant wear-out mechanism in modern insulated gate bipolar transistor (IGBT)-based power converters [4]. Thermomec fatigue stresses are caused by the operational thermal level and thermal cycling, whose mission profiles are generated by variable wind speeds and the Pulse-Width Modulation (PWM) caused alternating currents, for long-term and short-term thermal loadings.

Most of the articles on this subject only address the short-term thermal cycling stresses caused by periodic converter commutations [5]. However, some articles have suggested that long-term temperature cycles are more damaging, since the solders creep and crack propagation [6], [7]. Considering this fact, the authors in [8] have derived a multi-state reliability assessment model, which addresses the influence of long-term thermal cycling. In the proposed model, both the effect of wind speed and wind turbulence are taken into consideration. The pitfall of this article is that short-term thermal cycling is omitted. Ma et al. [9] considered different timespans of the thermal behavior in the WTPCS thermal loading profile. Thus, the lifetime of these power devices are estimated. In this article, most of the lifetime models are based on accelerating test results that can cover only limited ranges of amplitudes, durations, and maximum values of thermal cycles. In addition, some test conditions are difficult to implement. Taking this into consideration, the method proposed in [9] is hard to put forward into practical application. Comparatively, the FIDES [10] reliability guide is proposed based on a lot of industrial reliability data and several acceleration models. This guide considers technological and physical factors, precise mission profiles, and almost all of the thermal behavior in various timespans that are shorter than one year. Thus, it may be suitable for reliability evaluations of the power semiconductors used in variable wind speeds applications. Xie et al. [11] conducted some preliminary studies that referenced the FIDES guide in the reliability assessment of WTPCS. However, in this article only average wind speeds are considered, while the influence of wind turbulence is ignored. As a result, the obtained failure rate is lower than the actual value.

A reliability assessment model for the power semiconductors used in WTPCS is proposed in this paper. Four basic concepts contribute to this methodology:

1) Both long-term and short-term thermal behavior patterns contribute to the failure of power devices. Therefore, the thermal loadings under various timescales should be considered in the reliability assessment model.
2) In regards to long-term thermal loading, the influences of both wind speed and wind turbulence are considered. The operation state of WTPCSs is partitioned into different phases in terms of average wind speed and wind turbulence, which correspond to different stress levels. In addition, the randomly changing long-term thermal profile is processed using the rain-flow cycling count algorithm, which regulates thermal cycles. The average cycle information is then applied to calculate the failure rate that influences the factors of thermal loading and thermal cycling in each partitioned phase.
3) In regards to the short-term thermal loading, the wind profile is converted to a wind speed distribution, and the total failure rate is accumulated according to all of the wind speed contributions.
4) Finally, the failure rates assessed base on the long-term thermal loading and short-term thermal loading are added together to reflect the general performance of power devices.

The paper is organized as follows. Section II analyzes the timescale characteristics of thermal cycling in power devices under variable wind speed operation conditions. Section III proposes a reliability assessment model that considers the effect of long-term thermal behavior. Section IV presents a reliability assessment model that accounts for the influences of short-term thermal behavior. Section V demonstrates the reliability through a case study, and the influences of parameters such as cut-in, rated and cut-out wind speed to the failure rate are analyzed. Section VI concludes the study.

II. Thermal Behavior of WTPCSs Under Variable Wind Speed

Based on the principle analysis and the simulated thermal loading profiles under variable wind speeds [11], [12], the reasons for power device thermal loading can generally be classified into two different types from the timescale perspective:

1) Long-term thermal loading T_{j_L}, which varies with the mission profile of the wind speed as shown in Fig. 1. This roughly outlines the thermal loading profile.
2) By zooming in the image of the thermal mission profile in Fig. 1, the short-term thermal loadings are observed. This is caused by rapid and periodic alternations of load current in the converter, whose swing frequency is the fundamental frequency of the converter output. Under such a short time scale perspective, wind speed can be comparatively treated as a constant [16].

To sum up the aforementioned analysis of the reliability assessment model, two timescales of thermal cycling should be considered: long-term thermal cycling ΔT_{j_L}, which considers the influence of wind speed variations; and short-term thermal cycling ΔT_{j_S}, which accounts for the influence of alternating converter currents under a constant wind speed. Here different time-scale damages are independently accumulated. According to Miner's rule, the final fatigue damage can be concluded by linearly adding the different timescales of thermal loading contributions.

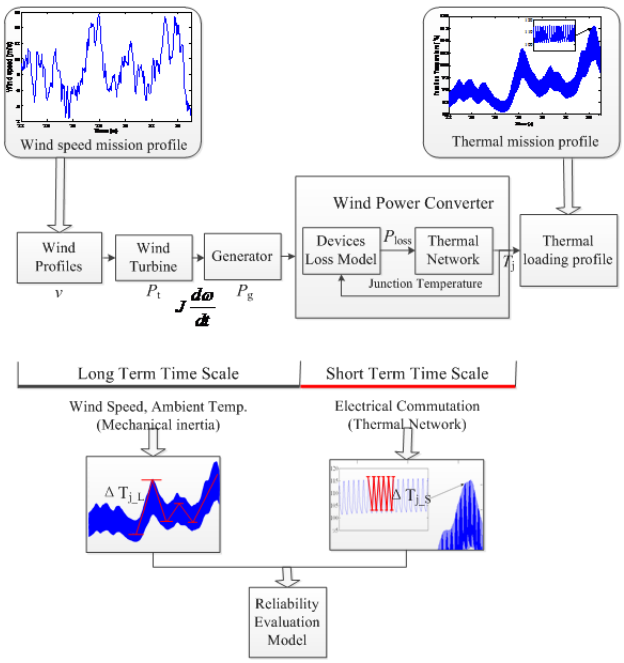

Fig. 1. Thermal mission profiles of power semiconductors in wind power converters under different time scales.

III. Profiles of Long-Term Thermal Loading and Reliability Evaluation

This section addresses long-term reliability assessment which is mainly caused by variations in wind speed. Considering the period for monsoon climate change is generally one year, one year's operation data is required to evaluate the influence of variable wind speed on the failure rate of power devices [2], [10], [11].

A. Generation of the Long-Term Thermal Loading Profile

To illustrate the general construction of a thermal loading profile, the thermal loading profile of power devices in the permanent magnetic synchronous generators (PMSG) of wind turbine power converters is calculated. The randomly changing thermal loading profiles are computed according to the values of wind speed samples. The full-scale output power of the wind power converter can be expressed as [11]:

$$P_{tj}=\begin{cases}0, & 0\le v_t<v_{ci}\\ (A+Bv_t+Cv_t^2)\times P_r, & v_{ci}\le v_t<v_r\\ P_r, & v_r\le v_t<v_{co}\\ 0, & v_{co}\le v_t\end{cases} \quad (1)$$

where P_r is the rated power of the wind turbine generator. The constants A, B, and C are denoted by v_{ci}, v_r, and v_{co},[20].

$$f_{gen}=\begin{cases}0 & 0\le v_t<v_{ci}\\ K_{fv}v_t & v_{ci}\le v_t<v_r\\ K_{fv}v_r & v_r\le v_t<v_{co}\\ 0 & v_{co}\le v_t\end{cases} \quad (2)$$

where $K_{fv}=p\lambda_{op}/2\pi R$; p denotes the pole pair numbers; λ_{op} is the tip speed ratio (TSR); and R is the radius of the wind turbine blade.

Based on the electromotive force equation $E=\sqrt{2}\pi NK_N\Phi f_{gen}$, the peak voltage of the PMSG can be written as:

$$U_{gen}=\begin{cases}0 & 0\le v_t<v_{ci}\\ K_{Uf}K_{fv}v_{to} & v_{ci}\le v_t<v_r\\ K_{Uf}K_{fv}v_r & v_r\le v_t<v_{co}\\ 0 & v_{co}\le v_t\end{cases} \quad (3)$$

where $K_{Uf}=\sqrt{2}\pi NK_N\Phi$; N denotes the winding turns; K_N is the winding coefficient; and Φ is the magnetic flux of each pole.

The conduction power losses of a diode and a IGBT can be given as [11]:

$$\begin{aligned}P_{IGBT}&=P_{cd,IGBT}+P_{sw,IGBT}\\ &=V_{ce0}\cdot I_{om}\left(\frac{1}{2\pi}\pm\frac{1}{8}M\cos\alpha\right)\\ &+r_{ce}I_{om}^2\left(\frac{1}{8}\pm\frac{M}{3\pi}\cos\alpha\right)\\ &+\frac{1}{\pi}f_{sw}(E_{on}+E_{off})\frac{V_{dc}\cdot I_{om}}{V_{ref,IGBT}\cdot I_{ref,IGBT}}\end{aligned} \quad (4)$$

$$\begin{aligned}P_D&=P_{cd,D}+P_{sw,D}\\ &=V_{f0}\cdot I_{om}\left(\frac{1}{2\pi}\mp\frac{1}{8}M\cos\alpha\right)\\ &+r_DI_{om}^2\left(\frac{1}{8}\mp\frac{M}{3\pi}\cos\alpha\right)\\ &\frac{1}{\pi}f_{sw}E_{SR}\frac{V_{dc}\cdot I_{om}}{V_{ref,D}\cdot I_{ref,D}}\end{aligned} \quad (5)$$

where f_{sw} denotes the switching frequency; E_{on} and E_{off} represent the energy losses in active and inactive states, respectively; V_{ref} and I_{ref} correspond to the rated voltage and current, respectively; E_{SR} represents the power loss in the diode conduction; cosα denotes the power factor; and M indicates the modulation index. The principle behind the use of "±" is that the top sign corresponds to the grid side converter and the bottom one is used on the generator side. I_{om} is the peak of the phase current on the grid side converter and can be approximated as:

$$I_{om\_gen}\approx\frac{2}{3}\frac{P_{tj}}{U_{gen}} \quad (6)$$

The mean value of the steady-state junction temperature is related to the total thermal resistance alone in this study. Fig. 2 depicts the model of the diodes and IGBTs.

In this figure, T_a, T_c, and T_h are the ambient, heat sink, and case temperatures, respectively; $T_{j,IGBT}$ and $T_{j,D}$ are the junction temperatures of the IGBT and the diode; $R_{thjc,IGBT}$ and $R_{thjc,D}$ are the junction-to-case thermal resistances for the IGBT and the diode, respectively; R_{thch} is the case-to-heatsink thermal resistance; and R_{thha} is the heatsink-to-ambient thermal resistance.

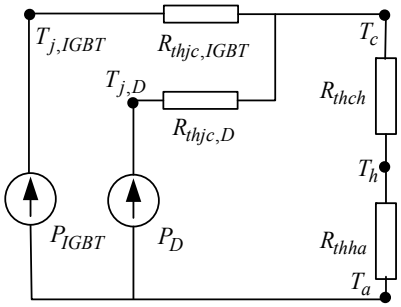

Fig. 2. Equivalent model of thermal resistance of the IGBT and the diode.

Based on the thermal resistance model, the junction temperature for the IGBTs and diodes can be expressed as:

$$\begin{cases} T_{j,T} = P_T \cdot R_{thjc,VT} + P_{loss} \cdot R_{thch} + P_{loss} \cdot R_{thha} + T_a \\ T_{j,D} = P_D \cdot R_{thjc,VD} + P_{loss} \cdot R_{thch} + P_{loss} \cdot R_{thha} + T_a \end{cases} \quad (7)$$

where P_{loss} denotes the total power loss of the IGBTs and the diodes.

B. Reliability Evaluation given Long-Term Thermal Loading

Wind speed and turbulence significantly affect the reliability of WTPCS power devices. Therefore, in this section, the operation state of a wind power converter is partitioned into different phases based on these two factors.

The probability of each state in a 2D multistate probability model of a WTPCS can be expressed as:

$$p(i,j) = \frac{t(i,j)}{T} \quad i = 2,\ldots,N_{\mathrm{Th}};\ j = 2,\ldots,N_{\mathrm{Cy}} \quad (8)$$

where $p(i, j)$ denotes the annual cumulative frequency of the (i, j)th state of the WTPCS at the ith average wind speed and the jth division of the wind turbulence intensity; t(i, j) represents the cumulative time for the states (i, j); T corresponds to the period considered, which is typically one year; and N_{th} and N_{Cy} are the division numbers for the average wind speed and wind turbulence intensity, respectively. The wind turbulence intensity is defined as the ratio of the standard deviation of wind speed to the average wind speed:

$$v_{tur} = \frac{\sigma}{v_{mean}} \quad (9)$$

where v_{tur} denotes the wind turbulence intensity; v_{mean} represents the average wind speed; and σ indicates the standard deviation of the wind speed for each hourly partitioned phase.

Based on FIDES, the thermal stress factor for the state (i, j) can be expressed as the Arrhenius law as:

$$\pi_{Thi} = \left(\frac{1}{S_{reference}} \times \frac{V_{applied}}{V_{rated}} \right)^p e^{11604 \times E_a \times [\frac{1}{293} - \frac{1}{(T_{mean\_i}+273)}]} \quad (10)$$

where $V_{applied}$ is the working voltage; V_{rated} is the rated voltage; $S_{reference}$ is the reference level for the electrical stress and p is the acceleration power for the electrical stress, which are both referred in the FIDES guide [10]; and E_a is the activation energy, where for different components the value is different. T_{mean_i} is the mean steady-state temperature of the components.

Based on the Norris—Landzberg acceleration model, the thermal cycling factor is written as:

$$\pi_{TCj} = \gamma \left(\frac{24}{N_0} \times \frac{N_{Cyj}}{t_j} \right) \times \left(\frac{\min(\theta_{cyj}, 2)}{\min(\theta_0, 2)} \right)^p \times \left(\frac{\Delta T_{cyj}}{\Delta T_0} \right)^n \times e^{1414 \times \left[\frac{1}{313} - \frac{1}{(T_{max\_cyj}+273)} \right]} \quad (11)$$

where t_j denotes the cumulative operation time for each state; N_0 and N_{cyj} represent the number of reference and actual temperature cycles for each state phase, respectively; θ_0 and θ_{cyj} are the reference and actual temperature cycle durations, respectively; ΔT_{Cyj} denotes the thermal amplitude of the cycle; T_{max_cyj} is the maximum thermal value of the cycle; and γ, p and n are specific constants that correspond to different types of components.

By combing the results of the partition of the WTPCS operation state and the FIDES philosophy regarding the assessment of multi-phase failure rates, the proposed failure rate calculation method for WTPCS power devices can be represented by:

$$\lambda_{com} = \sum_{i=1}^{N_{\mathrm{Th}}} \sum_{j=1}^{N_{\mathrm{Cy}}} \left[p(i,j) \times (\lambda_{0\mathrm{Th}} \cdot \pi_{\mathrm{Th}i} + \lambda_{0\mathrm{TC}} \cdot \pi_{\mathrm{TC}j}) \right] \times \pi_{\mathrm{in}} \times \pi_{\mathrm{Pm}} \times \pi_{\mathrm{Pr}} \quad (12)$$

where λ_{0Th} and λ_{0TC} denote the base failure rates of a component, which can be referred in the FIDES guide[10], both of which correspond to the thermal stress factor π_{ty} and the thermal cycling factor π_{TC}, respectively. π_{In} represents overstress, which is determined by the coefficient of sensitivity to the application field of the component; π_{Pm} indicates component quality; and π_{Pr} denotes the aging status in terms of the lifespan of a component, whose recommended value in a normal life stage is 4.

Based on the aforementioned analysis, Fig. 3 depicts the proposed reliability assessment diagram for the WTPCS. The procedure mainly includes the following steps:

1) Partition of the WTPCS Operation States: As suggested in Equ.(8), the process of partitioning the WTPCS operation states involves the following steps: a) The sampled time series wind speed data is divided into equivalent time-span segments. Each segment spans one hour as indicated by the FIDES. v_{mean} and v_{tur} should be calculated for each segment. b) These segments are then partitioned into N_{th} parts based on their minimum and maximum average wind speeds. c) For each segment based on the average wind speed, an advanced partition is conducted into N_{cy} parts based on a wind turbulence value that ranges from the minimum to the maximum value. As a result, the WTPCS operation state is divided into $N_{th} \times N_{cy}$ parts. d) The cumulative operation time t(i, j) for each $N_{th} \times N_{cy}$ of the parts is also recorded to calculate the occurrence frequency p(i, j) for each state.

2) Calculation of the Thermal Loading Profiles of the Power Devices: The power losses can be calculated using Equs.(1)-(5)

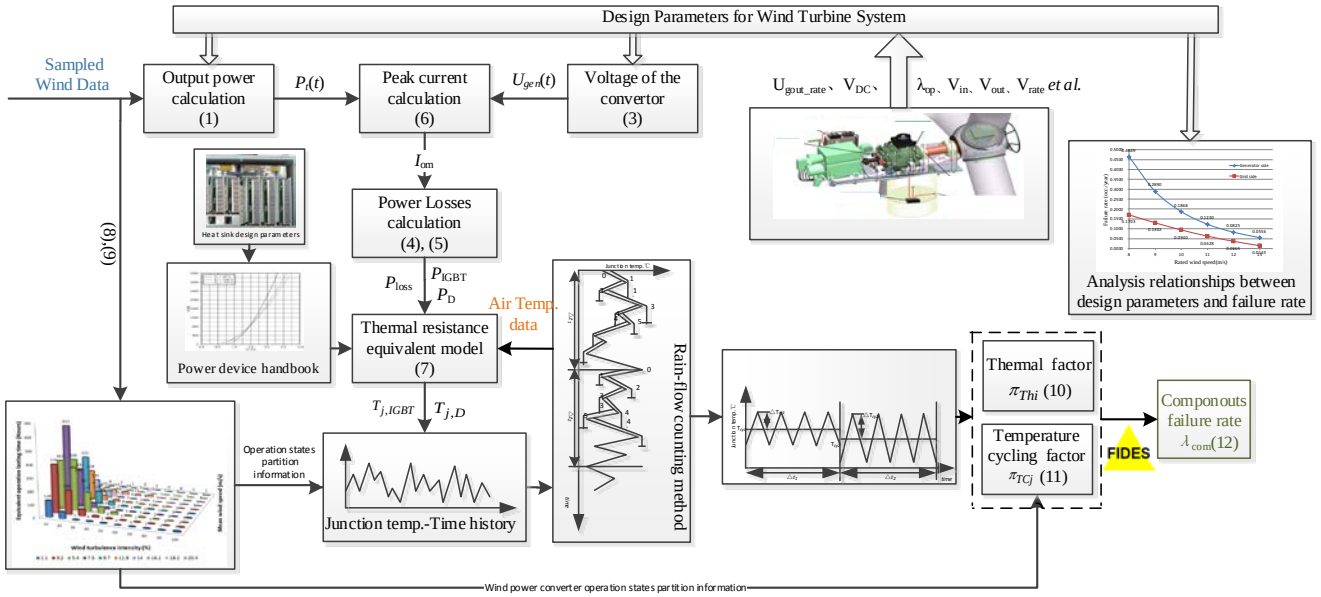

Fig. 3. Schematic of the assessment of power device reliability induced by long-term thermal cycling.

based on the sampled wind speed. The thermal loading profile can then be computed with Equ. (7).

3) Regulation of the Random Thermal Loading Profile using the Rain-flow Cycling Count Algorithm: As shown in Equ. (11), the thermal cycling factor in each separate phase of the WTPCS operation state is affected by ΔT_{cyj} and T_{max_cyj} as well as the duration time θ_{cyj} and cycle values N_{cyj}. Thus, the cycle counting method must be applied to extract the regular thermal cycling information from the randomly changing thermal profile. The rain-flow algorithm is a popular method for cycle counting. Fig. 4 displays the process when the rain-flow algorithm is used to regulate the randomly changing thermal profiles for each partitioned phase of the WTPCS operation. The average thermal value T_i, cycle number N_{cyj}, amplitude ΔT_{cyj}, maximum value T_{max_cyj}, and duration time θ_{cyj} are computed for each phase. These values are the arguments in the calculation of the failure rate thermal factor π_{th} in Equ. (10) and of the thermal cycling factor π_{cy} in Equ. (11).

4) Failure Rate Calculation: The failure rate of a power device can be determined using Equ. (12) based on the partition results $p(i, j)$, the failure rate thermal factor π_{th}, and the thermal cycling factor π_{cy}.

IV. Profiles of the Short-Term Thermal Loading and Reliability Evaluation

As indicated in Fig.1, this type of thermal loading is mainly caused by alternating currents in the power converter that change periodically. This variation is observed even under the constant wind speeds that are omitted in the long-term thermal loading profile. As a result, the thermal cycling information should be extracted from a zoomed in perspective with a more detailed model. In this section, a reliability assessment model that considers short-term thermal behavior is established.

A. Characteristics and Thermal Profile of Short-term Thermal Loading

The amplitude of the short-term thermal loading is lower than that of the long-term thermal loading. However, the oscillation frequency is much higher than the long-term thermal cycling. The simulation results indicate that the mean junction temperature and temperature fluctuations are constant under stable operating states over the entire wind speed range [16]. Thus, the thermal cycling information regarding the mean junction temperature, temperature fluctuation, and cycling duration can be calculated at different wind speeds and can be directly applied to the FIDES model of failure rate without the rain-flow counting.

The mean temperature of the thermal cycling can be computed using the analytical functions of Equs. (1)-(7). The cycling duration θ_{cyj} represents half of the oscillation cycle, which can be determined with Equ.(2). The cycling amplitude ΔT_{cy} can be calculated as in [16]:

$$\Delta T_{cy} = P_{loss} \cdot Z_{th}\left(\frac{3}{8 f_0}\right) + 2P_{loss} \cdot Z_{th}\left(\frac{1}{4 f_0}\right) \qquad (13)$$

where Z_{th} is the thermal impedance in the datasheet of the power device; and f_0 is the fundamental frequency of the converter output. At the grid side, this frequency is 50Hz. Meanwhile, that on the generator side can be calculated using Equ.(2).

B. Reliability Evaluation Given Short-Term Thermal Loading

In this subsection, the reliability assessment model of the multi-average wind speed is introduced in consideration of

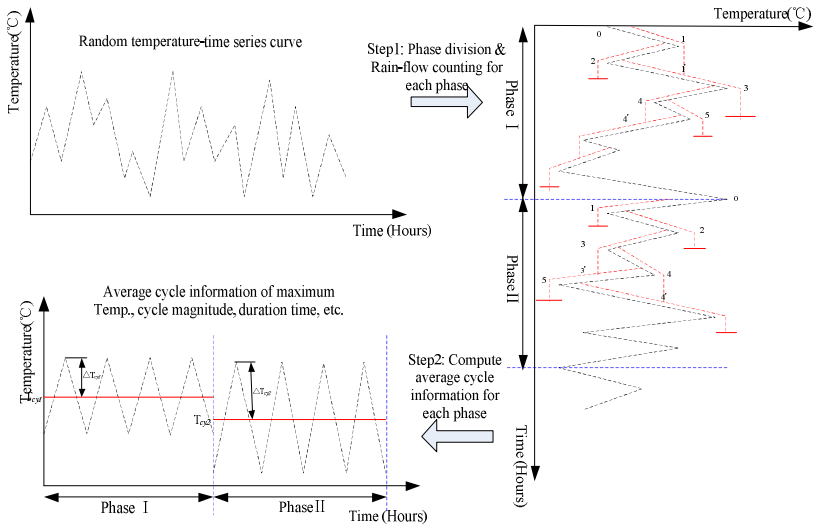

Fig. 4. Rain-flow cycle counting algorithm in relation to junction temperature.

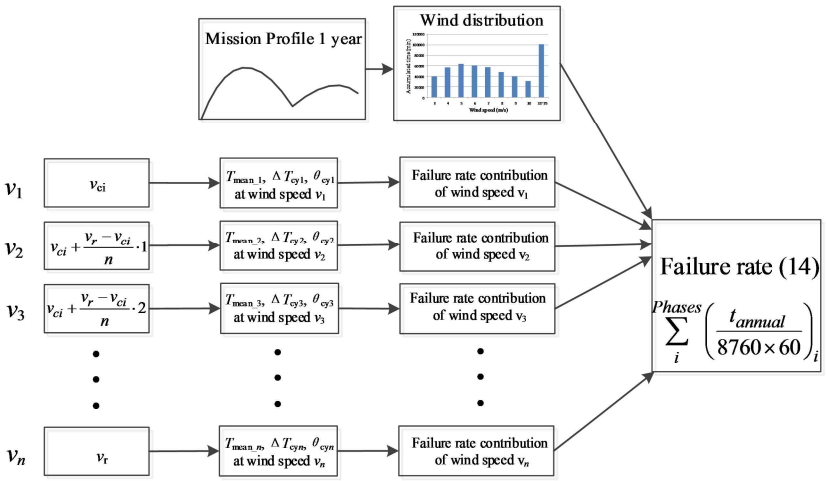

Fig. 5. Schematic of the assessment of power device reliability induced by short-term thermal cycling.

the fact that the cycling information of the short-term thermal loading varies with the wind speed. According the FIDES guide, the failure rate can be calculated as:

$$\lambda_{com} = \sum_{i}^{Phases} \left(\frac{t_{annual\_i}}{8760 \times 60} \right)_i \times (\lambda_{0\mathrm{Th}} \cdot \pi_{\mathrm{Th}i} + \lambda_{0\mathrm{TC}} \cdot \pi_{\mathrm{TC}i}) \times \pi_{\mathrm{in}} \times \pi_{\mathrm{Pm}} \times \pi_{\mathrm{Pr}} \quad (14)$$

where t_{annual_i} denotes the accumulated time for each wind speed distribution phases.

As presented in Fig. 5, the reliability assessment flow generated by the short-term thermal loading differs from that induced by the long-term thermal loading. The long-term thermal loading changes with variable wind speeds. Meanwhile, the short-term thermal loading is caused by alternating converter currents, the amplitude and mean junction temperature of which are related to the average wind speed. The reliability assessment caused by the short-term thermal loading involves three main steps:

1) The thermal cycling information of T_{mean}, ΔT_{Cy}, and θ_{cy} at different wind speeds that range from the cut-in to the rated wind speed. This cycling information is then used to compute $\pi_{\mathrm{th}i}$ and $\pi_{\mathrm{cy}i}$ in Equs. (10) and (11), respectively.
2) The time series wind profile for one year is converted into a wind speed distribution. Specially, wind speeds that are greater than the rated value and smaller than the cut-out value are transferred in the range of the rated wind speed.
3) Based on the result of the wind speed distribution, which denotes each phase accumulation time t_{annual_i}, and the $\pi_{\mathrm{th}i}$ and $\pi_{\mathrm{cy}i}$ values for each phase, the failure rate of the power device can finally be determined using Equ.(12).

V. Case Study

To apply the proposed reliability assessment method, a typical field-sampled wind speed and a wind turbine system are established for a case study. The parameters of the WECS

TABLE I
WECS PARAMETERS

Rated power (MW)	2.5
Cut-in wind speed (m/s)	3
Rated wind speed (m/s)	11
Cut-out wind speed (m/s)	25
Rotor blade diameter (m)	90
Rated rotor speed (rad/s)	1.9
Rated rotor torque (N·m)	3.0×10^6
Total inertia of the wind turbine (kg·m^2)	2.0×10^7
Air density (kg/m^3)	1.225
Power coefficient C_{pmax}	0.593
Grid voltage (V)	690
Grid frequancy (Hz)	50
IGBT switching frequency (Hz)	3000
DC link voltage (V)	1100

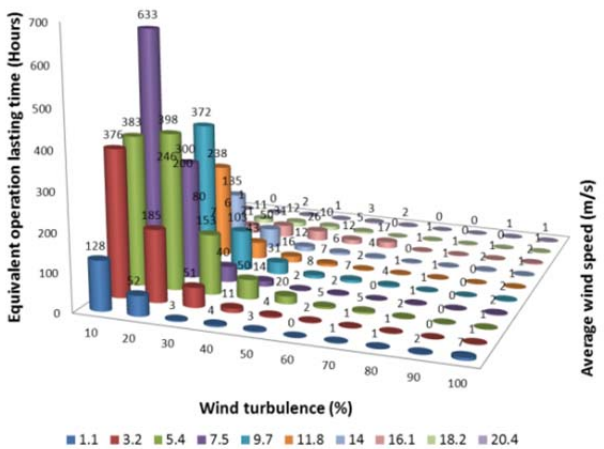

Fig. 6. Distributions of wind speed and wind turbulence intensity.

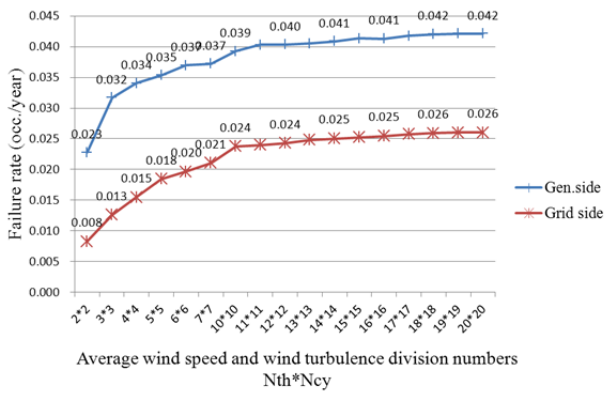

Fig. 7. Results of power device reliability assessment as induced by long-term thermal cycling under different average wind speeds and wind turbulence division numbers.

are presented in Table I, and the information on the main components are presented in the Appendix.

A. Reliability Assessment under Long-Term Thermal Loading

The WTPCS operation states are partitioned as shown in Fig. 6, the result shows that most of the states are centered on the point of the average wind speed 7.5m/s and the wind turbulence intensity 10%.

The effect of the operation state partition numbers N_{th} and N_{cy} on the WTPCS failure rate is investigated as depicted in Fig. 7. When N_{th} and N_{cy} reach a certain level, the failure rates of the power devices stabilize at approximately 0.042 and 0.026 occ./year on the generator side and grid sides, respectively. Conceptually, larger partition numbers generate more accurate results, but require additional calculation time. Fig. 7 indicates that both N_{th} and N_{cy} can be set at 20.

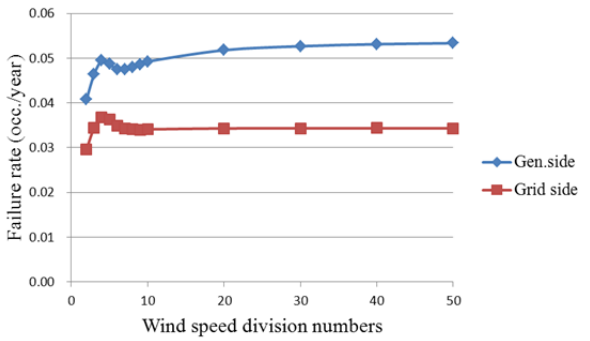

Fig. 8. Results of power device reliability assessment as induced by short-term thermal cycling under different wind speed division number.

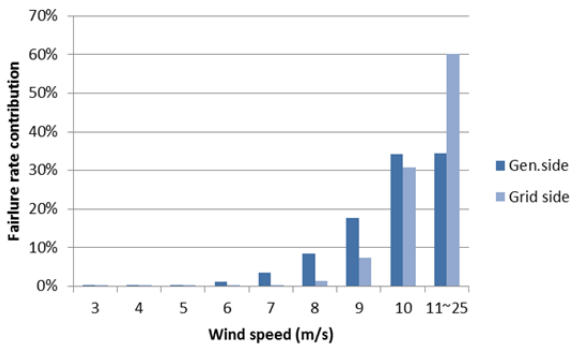

Fig. 9. Failure rate contribution of different wind speeds.

B. Reliability Assessment under Short-Term Thermal Loading

Using the proposed approach for power device reliability assessment based on short-term thermal loading, the failure rate calculation results are shown in Fig. 8. The power devices in the generator side and grid side finally stabilize at 0.053 occ./year and 0.034 occ./year, respectively. The wind speed division number can be set as 50 to get the table results.

The contributions of different wind speeds to this failure rate are plotted in Fig. 9. As Fig. 9 shows, wind speeds around the rated value contribute the most to this failure rate, since the converter power losses at around rated operation state are significant. Furthermore, the contribution of the rated wind speed for the generator side power device is larger than the grid side, which occupies 60% of the total failure rate. This finding is ascribed to the fact that at the grid side,

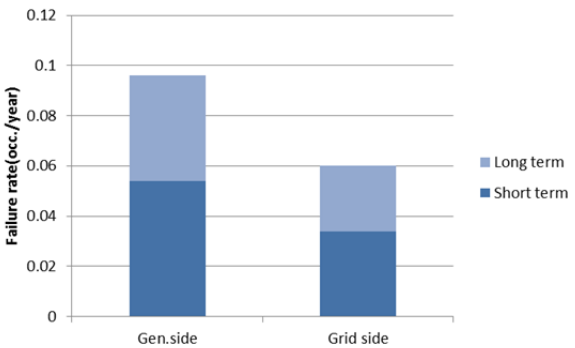

Fig.10. Assessment result of total power device failure rate given different timescales of thermal loading.

the converter output power variation is partially smoothened by the direct current (DC)-link capacitors.

C. Assessment Result of the Total Power Device Failure Rate

Fig. 10 displays the total failure rate of a power device by summing up the contributions of the short-term and long-term thermal behaviors. The total failure rates for the generator and grid sides are 0.096 and 0.060 occ./year, respectively. The long-term and short-term thermal loading are compared in terms of their contributions, as indicated in Fig. 10. The short-term thermal loading contributes more than the long-term thermal loading because its cycling numbers are significantly larger even though its cycling amplitude is smaller, as indicated in Fig.1.

D. Effects of WECS Parameters on the Failure Rate of WTPCS Power Devices

To accommodate the distribution of different wind speed resources, the WTPCS manufacturers may set various cut-in, rated, and cut-out wind speeds. In [19], these WECS parameters are investigated in different farms, and the results show that the cut-in wind speed is generally $0.6v_m$, the rated wind speed ranges from $1.6v_m$ to 1.75 v_m, and the cut-out wind speed is generally set at $3v_m$. In this case, v_m is the annual mean wind speed. As stated in Section III, these parameters are directly related to the power loss, junction temperature, and power device failure rate. Hence, this section analyzes the effects of WECS parameters on the failure rate of WTPCS power devices based on the aforementioned reliability assessment model.

The relationship between the cut-in wind speed and the reliability of WTPCS power devices is determined as shown in Fig. 11, where the cut-in wind speed is varied, and the other parameters remain constant. The failure rate decreases as the cut-in wind speed increases, and this effect can be primarily attributed to the fact that the WTPCS standby time increases with a cut-in wind speed increase.

Fig. 13 presents the effect of the cut-out wind speed on the reliability of WTPCS power devices when the cut-out wind

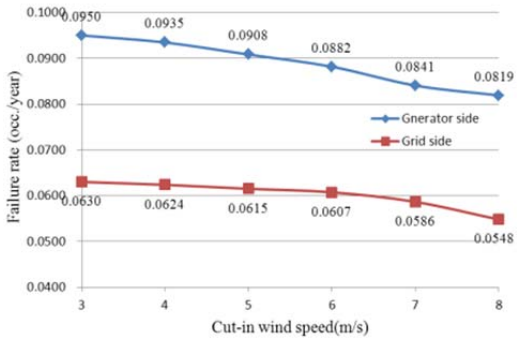

Fig. 11. Effect of the cut-in wind speed of wind turbines on the failure rate of WTPCS power devices.

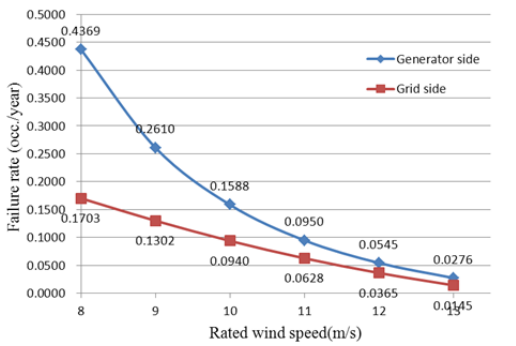

Fig. 12. Effect of the rated wind speed of wind turbines on the failure rate of WTPCS power devices.

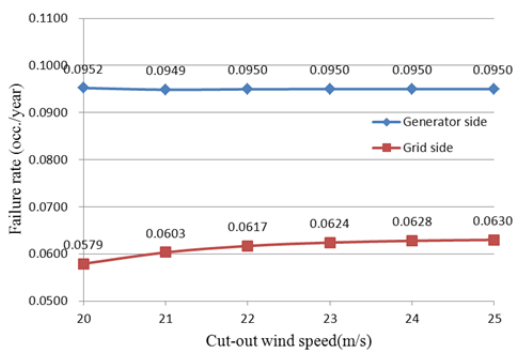

Fig. 13. Effect of the cut-out wind speed of wind turbines on the failure rate of WTPCS power devices.

speed varies. This effect may be complicated. The reliability of the generator side remains almost stable, whereas the grid side increases. To trace the influential contributors, two factors that contribute opposite effects on the failure rate are considered: the first is that an increase in the cut-out speed implies a prolonged annual operation time, which may cause the failure rate to be higher; the second is that an increase in the cut-out speed also implies a fewer frequently cut-in and recut-in behaviors, which corresponds to a variation in the junction temperature from the rated stress level to a circumstance temperature. As a result, these two factors balance out in the generator side converter. Meanwhile, in the grid side converter, the DC link flattens the variation. Therefore, the first influential factor is dominant.

To conclude, the effect of the rated wind speed on the failure rate is stronger than those of the cut-in and cut-out wind speeds.

VI. CONCLUSION

In this study, a failure rate assessment model is proposed for WTPCS power devices. This model considers thermal behavior at different timescales. For the assessment of long-term thermal loading, the operation state of the WTPCS is partitioned into different phases in terms of average wind speed and wind turbulence intensity, which correspond to different thermal factors and thermal cycling factors. Therefore, the contributions of these phases to reliability are considered. The feature of this model is that it considers both the influences of the average wind speed and the wind turbulence intensity. For short-term thermal loading, the wind profile is first converted into a wind speed distribution. The contributions of different wind speeds on the failure rate are then calculated. A multi-state reliability assessment model is then developed with the proportional addition of the different failure rate contributions. With the establishment of the failure rate assessment model, the influences of cut-in, rated, and cut-out wind speeds on the failure rate of the WTPCS power devices can be acquired. Among these factors, the rated wind speed has the greatest impact on the failure rate.

APPENDIX

For IGBT modules: type FZ2400-R17KE3; V_{rated}: 1700V; I_{rated}:2400A; rated saturation voltage drop V_{CEsat}: 1.9V; voltage drop V_{CE0}: 0.81V; E_{on} and E_{off}: 1070mJ; E_{on} and E_{off} for Diode: 390mJ; R_{thjh} for IGBT: 19K/kW; R_{thjh} for Diode: 44K/kW; R_{thha}: 0.454K/kW; IGBT package type: ISOTOP; λ_{0TC} for IGBT: 0.3021; λ_{0TC} for Diode:0.1574; p_{case}: 0; p_{solder}: 1/3; n_{case}: 4; n_{solder}: 1.9; λ_{0TC_case}: 0.03333; λ_{0TC_joint} : 0.1665; π_{Pm}: 0.75; π_{Pr}: 4;π_{in}: 3; γ: 1.4.;E_a:0.7; $S_{reference}$:1; p:2.4

ACKNOWLEDGMENT

This research work was supported by the International Science & Technology Cooperation Program of China (No.2013DFG61520), the National Natural Science Foundation of China (No.51377184), the Fundamental Research Funds for the Central Universities (No.CDJZR12150074), the Science & Technology Research Program of Chongqing Municipal Education Commission (No.KJ1501010), the Integration and Demonstration Program of Chongqing, China (No.CSTC2013JCSF70003), the Chongqing University Innovation Team Founding (No.KJTD201320).

REFERENCES

[1] F. Blaabjerg, M. Liserre, and K. Ma, "Power electronics converters for wind turbine systems," *IEEE Trans. Ind. Appl.*, Vol. 48, No. 2, pp. 708-719, Mar. 2012.

[2] F.Spinato, P. J. Tavner, G. J. W. van Bussel, and E. Koutoulakos, "Reliability of wind turbine subassemblies," *IET Renewable Power Generation*, Vol. 3, No. 4, pp. 1-15, Dec. 2009.

[3] P. Tavner, *Offshore wind turbines relaibility avilability & maintenance*, Instituttion of Engineering and Technology, London, United Kingdom, pp.243-253, 2012.

[4] S.Yang, D. Xiang, A. Bryant, P. Mawby, L. Ran, and P. Tavner."Condition monitoring for device reliability in power electronic converters: A review," *IEEE Trans. Power Electron.*, Vol. 24, No. 11, pp. 2734-2752, Nov. 2010.

[5] A. Isidor, F. M. Rossi, and F. Blaabjerg, "Thermal loading and relaibility of 10 MW multilevel wind power converter at different wind roughness classes," *Energy Converesion Congress and Exposition (ECCE)*, pp. 2172-2179, 2012.

[6] M. Arifujjaman, M. T. Iqbal, and J. E. Quaicoe. "Reliability analysis of grid connected small wind turbine power electronics," *Applied Energy*, Vol. 86, No. 9, pp. 1617-1623, Sep. 2009.

[7] G. Yang, *Life Cycle Reliability Engineering*, John Wiley & Sons, Inc., Hoboken, New Jersey, p. 247, 2007.

[8] H. Li, H. T. Ji et. al., "Reliability evaluation model of wind power converter system considering variable wind profile", *IEEE Energy Conversion Congress and Exposition (ECCE)*, pp. 3051-3058, 2014.

[9] K. Ma, M. Liserre, and F. Blaabjerg, "Lifetime estimation for the power semiconductors considering mission profiles in wind power converter," *IEEE Energy Conversion Congress and Exposition (ECCE)*, pp. 2962-2971, 2013.

[10] Reliability Methodology for Electronic Systems , *FIDES guide2009,*http://fides-reliability.org/files/UTE_Guide_FIDES_2009_Ed_A_EN.pdf, 2015.

[11] K. G. Xie, Z. F. Jiang, and W. Y. Lim "Effect of wind speed on wind turbine power," *IEEE Trans. Energy Convers.*, Vol. 27, No. 1, pp. 96-104, Mar. 2012.

[12] K. Ma, M. Liserre, F. Blaabjerg, "Reactive power influence on the thermal cycling of multi-MW wind power inverter," *Proceedings of the 27th Annual IEEE Applied Power Electronics Conference and Exposition (APEC)*, pp. 262-269, 2012.

[13] H. Huang, P. A. Mawby, "A lifetime estimation technique for voltage source inverters", *IEEE Trans. Power Electron.*, Vol. 28, No. 8, pp. 4113-4119, Aug. 2013.

[14] K. Ma, M. Liserre, F. Blaabjerg, and T. Kerekes, "Thermal loading and lifetime estimation for power device considering mission profiles in wind power converter", *IEEE Trans. Power Electron.*, Vol. 30, No. 2, pp. 590-602, Feb. 2015.

[15] J. Morren, J. Pierik, S.W.H. de Haan, "Inertial response of variable speed wind turbines," *Electric Power Systems Research*, Vol. 76, No. 7, pp. 980-987, Jul. 2006.

[16] D. Zhou, F. Blaabjerg, M. Lau, and M. Tonnes, "Thermal analysis of multi-MW two-level wind power converter," *4thIEEE International Symposium on Power Electronics for Distributed Generation Systems (PEDG)*, pp. 5858-5864, 2013.

[17] F. Casanellas, "Losses in PWM inverters using IGBTs," *IEE Proc. Electric Power Applications*, Vol. 141, No.5 , pp. 235-239, 1994.

[18] IEC 61400-1: 2005 *Wind Turbines-Part 1: Design Requirements*. Geneva, Switzerland: International Electrotechnical Commission.

[19] S. H. Jangamshetti and V. G. Rau, "Site matching of wind turbine generators: a case study," *IEEE Trans. Energy Convers.*, Vol. 14, No. 4, pp. 1537-1543, Dec. 1999.
[20] P. Giorsetto and K. F. Utsurogi, "Development of a new procedure for reliability modeling of wind turbine generators," *IEEE Trans. Power App. Syst.*, Vol. PAS-102, No. 1, pp. 134-143, Jan. 1983.

Haiting Ji received her B.S. degree in Electrical Engineering from Yanshan University, Qinhuangdao, China, in 2010; and her M.S. degree in Electrical Engineering from Chongqing University, Chongqing, China, in 2014. She is presently working at Chongqing Three Gorges University, Chongqing, China. Her current research interest include power electronics converters, and their control and reliability in wind power generation.

Hui Li received his M.S. and Ph.D. degrees in Electrical Engineering from Chongqing University, Chongqing, China, in 2000 and 2004, respectively. In 2000, he joined the Department of Electrical Engineering, Chongqing University, where he is presently working as a Professor. In 2005, he joined the Institute of Energy Technology, Aalborg University, Aalborg, Denmark, as a Visiting Researcher and later as a Postdoctoral Researcher. His current research interests include renewable energy systems and distributed generation.

Yang Li received his B.S. degree in Electrical Engineering from Sichuan Agricultural University, Sichuan, China, in 2013. He has been working towards his M.S. degree in the Department of Electrical Engineering, Chongqing University, Chongqing, China, since 2013. His current research interests include wind power converter reliability and control strategies for large integrated wind farms.

Li Yang has been working towards his B.S. degree in the Department of Electronics and Information Processing, Chongqing Three Gorges University, Chongqing, China, since 2012. He is currently doing his internship at Chongqing kk-Qianwei Windpower Equipment Co., Ltd., Chongqing, China.

Guoping Lei received his M.S. degree in Communication and Information from Chongqing University, Chongqing, China, in 2009. Since 2009, he joined has been with Chongqing Three Gorges University, Chongqing, China, where he is presently working as an Associate Professor. His current research interests include data digging and processing.

Hongwei Xiao received his B.S. degree in Electrical Engineering from Chongqing University, Chongqing, China, in 2014. He has been working towards his M.S. degree in the Department of Electrical Engineering, Chongqing University, Chongqing, China, since 2015. His current research interests include power electronics reliability and control strategies.

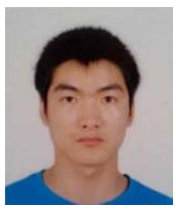

Jie Zhao received his B.S. degree in Electrical Engineering from Chongqing University, Chongqing, China, in 2014. Since 2015, He has been working towards his M.S. degree in the Department of Electrical Engineering, Chongqing University, Chongqing, China, since 2015. His current research interests include wind power converter reliability and control strategies.

Lefeng Shi received his M.S. and Ph.D. degrees in Technical Economics and Management from Three Gorges University, Hubei, China, in 2009 and 2012, respectively. His current research interests include data analysis and product reliability management.